17th World Conference on Earthquake Engineering, 17WCEE

Sendai, Japan - September 13th to 18th 2020

ASSESSING REPARABILITY OF DAMAGED BUILDINGS BASED ON IMPAIRMENT OF FUTURE EARTHQUAKE PERFORMANCE

P. B. Murray[(1)], A. B. Liel[(2)], K. Elwood[(3)], Z. Bullock[(4)]

[(1)] *Ph.D Student, University of Colorado Boulder, barbara.murray@colorado.edu*
[(2)] *Associate Professor, University of Colorado Boulder, abbie.liel@colorado.edu*
[(3)] *Professor, University of Auckland, k.elwood@auckland.ac.nz*
[(4)] *Ph.D Candidate, University of Colorado Boulder, zachary.bullock@colorado.edu*

Abstract

This study proposes a framework for the assessment of the performance of reinforced concrete (RC) buildings following significant earthquakes. Of particular interest is the effect of damage in changing in a structure's capacity to withstand future shaking events.

First, nonlinear three-dimensional models representative of a RC building of interest are developed in *OpenSees* and subjected to an initial incremental dynamic analysis (IDA) to develop a discrete set of initial damage conditions. Following each dynamic analysis, a static pushover is run to quantify loss of strength, stiffness, and deformation capacity from the ground motion. A representative subset of the initial damage conditions is selected using particle swarm optimization to be used in subsequent analyses. The selection criteria used to identify these conditions includes strength, stiffness, deformation capacity, and residual drift. Subsequent analyses are employed to assess the performance of the damaged building at target shaking intensities that correspond to serviceability, design earthquake (DE), and maximum considered earthquake (MCE) demands. In each subsequent analysis, the building is first subjected to an initial motion that replicates the initial damage condition, and then a second motion at a target performance level.

The drift demands in the damaged building are compared to those in the undamaged building, and the results of these analyses are used to create a model indicating what damage in the first motion is so severe that it impairs performance. Trends between metrics of the initial damage condition and change in demand are observed.

This process begins with results from the initial set of initial damage conditions, which are used to develop a model of which points are most informative. Additional initial damage condition cases are selected using a random forest to predict which points will be most informative in the model.

An example building model representing a modern, ductile RC frame was analyzed using this framework. For this ductile building, substantial damage could be incurred in a first motion before impairing even serviceability performance. The damage level at which performance was affected increased with the shaking intensity of the subsequent motion (i.e., the change in performance in at serviceability levels happens at lower damage than the change at MCE levels). Peak story drift was the most strongly correlated indicator of subsequent performance at all shaking intensities.

Keywords: incremental dynamic analysis; post-earthquake performance; machine learning; RC structures

1. Introduction

This study proposes and illustrates a framework for the assessment of post-earthquake performance of reinforced concrete (RC) structures. We are particularly interested in identifying those measures of damage which most strongly correlate with performance in subsequent earthquake events, and what levels of damage compromise future performance.

This information can be used to guide decision-making for post-earthquake building assessment. Repair decisions depend on a number of factors, including level of damage, expected performance in a future event, feasibility of repair and retrofit, safety perception and codes and standards [1]. We identify three conditions a building may be in following an earthquake. First, the building may have sufficient capacity to resist subsequent shaking. Second, a building may require repair to return to satisfactory capacity. Third, the building may be damaged past feasible repair, and need to be demolished. We have chosen to focus on RC buildings because this type of construction is common in the US and abroad, and the quantitative distinctions between these categories are unclear. Damage in RC buildings is less discretized than in steel counterparts; instead, a spectrum is possible. Marder et al. [2] studied the relationship between deformation demands, observable damage (i.e. cracks), and residual stiffness, and found that observable damage did not always correlate strongly with residual stiffness of a plastic hinge. Also, yielding of longitudinal reinforcement may not be observable, and, due to axial loads, columns may appear undamaged, despite significant peak demands [2]. In addition, significant losses and downtime resulting from damage to structural and non-structural components can occur even in code-conforming RC buildings [2,3]; in Christchurch, New Zealand, for example, approximately 65% of "significant" RC buildings—commercial and residential buildings more than 5 stories tall—were torn down after the earthquake[1]. Post-earthquake decisions are, in reality, highly influenced by non-engineering factors such as repair costs, risk perceptions, changes to building code requirements and insurance costs [1], but our focus is on structural engineering factors that affect decisions. Indeed, Elwood et al. [4] reflected that limitations on the residual capacity of concrete structures and elements also contributed to conservative estimations of future performance [4].

A focus of this effort is to develop strategies to assess of performance of an earthquake-damaged building while avoiding the computationally intensive nature of "back-to-back" analysis. This type of analysis requires running many ground motions for the undamaged building and then a subsequent analysis of the damaged building, resulting in significant computational time [5]. Accordingly, we employ optimization algorithms and machine learning methods to identify a subset of analyses that well-represent the possible damage conditions for a structure. Classification and prediction learning methods are adopted to identify additional analyses that will improve the results.

This paper outlines the preliminary development of the framework, and results from an example building. This building was developed to represent a modern, ductile RC frame building in California.

1.1 Review of previous work

Previously, researchers have observed the change in collapse capacity and drift demands of damaged, modern RC frame buildings (in comparison to an undamaged building). For example, Raghunandan et al. [5] found that, for modern well-detailed ductile RC frame buildings, drift demands in subsequent events do not increase until the mainshock or first event peak story drift exceeds 2%. Hosseinpour and Abdelnaby [6] observed a 20% change in collapse capacity associated with demands at "life safety" levels in a first event. Zhang et al. [7] quantified changes in collapse capacity associated drift demands in a first (damaging) motion showing: a 7% reduction in collapse capacity for a building damaged at 1% drift, and a 40% reduction when the building was damaged at 3% drift. In a study of aftershock collapse fragilities of older, less ductile, RC buildings, Jeon et al. [8] observed a shift in the collapse fragility when drift exceeded 1.2% in an initial motion. Similarly, Ryu and Luco [9] found that 3.5% drift corresponds with a 25% reduction in capacity.

Researchers who have studied mainshock-aftershock performance of modern steel frame buildings observed similar thresholds as to when damage significantly matters. For example, Ruiz-García and Aguilar [10] studied the change in performance associated with residual drift demands from the first motion, and

showed that the median spectral acceleration (Sa) at which the demolition threshold is reached is reduced by 10% if the building retained residual drifts of 1.4%. Li and Song [11] found that "moderate damage", or approximately 2.5% peak drift, leads to a 20% reduction in collapse capacity for modern steel buildings.

Researchers who have studied the effect of ground motion duration have observed similar trends in performance. Fairhurst et al. [12] observed that RC shear wall buildings experienced comparable peak displacements and peak forces, but higher energy demands during motions with longer durations. They note that the number and amplitude of cycles most strongly affect response. Similarly, Raghunandan and Liel [13] studied the change in collapse capacity of structures under long duration shaking, and found that long duration events decrease the collapse capacity of RC buildings by 26 - 56%, and that the change depends on the ductility capacity and period of the structure. Chandramohan et al. [14] also observed a decrease in collapse capacity of 17% in steel buildings subjected to long duration motions.

These studies have also indicated what characteristics of buildings may influence these conclusions. Mahin [15] found that structures that were relatively weak and had short periods were more likely to develop significant inelastic deformations and be more vulnerable to large drift demands to subsequent events. Uma et al. [16] showed that the building's period affected response. Amadio et al. [17] found that highly ductile structures do not see a significant "penalty" when subjected to repeated events, though structures with less ductility do. Raghunandan et al. [5] showed that buildings that were more susceptible to P-delta effects were resultingly more sensitive to mainshock damage. Most of these studies have been for structures without significant irregularities.

2. Framework overview

The proposed framework (Fig. 1) uses nonlinear dynamic analysis to assess the impact of damage sustained during ground shaking on the post-earthquake performance of a building. Post-earthquake performance, here, refers to the ability of a damaged building to resist subsequent shaking and meet specified performance goals.

Incremental dynamic analysis (IDA) is first used to produce a set of initial damage conditions (IDC) (Box 1.2). This analysis is used to define the response of a building that result from a range of earthquake events. We consider damage metrics related to drifts and changes to strength, deformation capacity, and stiffness. The effect of this damage is quantified through a suite of "back-to-back" analyses applied to a subset of IDCs that have been selected using an optimization algorithm (Box 2.1.1) In these back-to-back analyses, a first ground motion is applied to replicate the IDC, followed by a second, scaled motion that is used to assess whether the building meets various performance targets (Box 2.2.1). These scaled motions are also applied to the undamaged building (Box 2.2.2), and the change in drift demand between the undamaged and damaged building state is determined (Box 2.3). This response is summarized as the median change in demand over the suite of motions applied to a building at a single damage state.

This framework focuses on the drift response of the structure at target (i.e., serviceability, MCE and DE) levels. We are interested in drifts because they are strongly correlated with seismic performance metrics like economic losses [18]. We fit a bilinear regression model to these data that show the relationship between increased initial damage and drift demand (Box 2.4). The "corner" in the bilinear model is used to identify at what levels of damage performance in the subsequent is compromised. In addition, the bilinear regression model is used to select additional IDCs for further analysis (Box 3.1, 3.2.1, 3.3, 3.4), identifying which IDCs will be most informative in quantifying when damage matters.

3. Illustrative building example

We illustrate this framework with a three-story modern RC building designed and detailed for seismic loading in California. We chose to begin with a modern RC frame building because, while these buildings tend to protect life safety, the type of damage sustained can lead to significant loss and downtime and, thus, repair decisions can be important [2,3]. Further, a ductile building tends to lose capacity more gradually rate than a brittle building, where performance in a subsequent event drops more precipitously.

In this illustrative example building, the bays are 5 m wide, and each story is 3 m tall. The plan view is shown in Fig. 2a. The beam-column strength ratio is 1.4 for typical beam-column joints. From eigenvalue analysis, the (undamaged) building's natural period is 1.0 s in both directions. The space frame building has a deformation capacity of 7 (quantified as the ratio between post-peak displacement at 80% of peak strength and yield strength from [19]). Fig. 2c shows the response of the undamaged building during a static pushover analysis in the weaker direction under a triangular lateral load. This pushover shows that the lateral building strength (V/W = 0.24 g), initial stiffness and deformation capacity are comparable with modern RC frames designed by Haselton et al. [20].

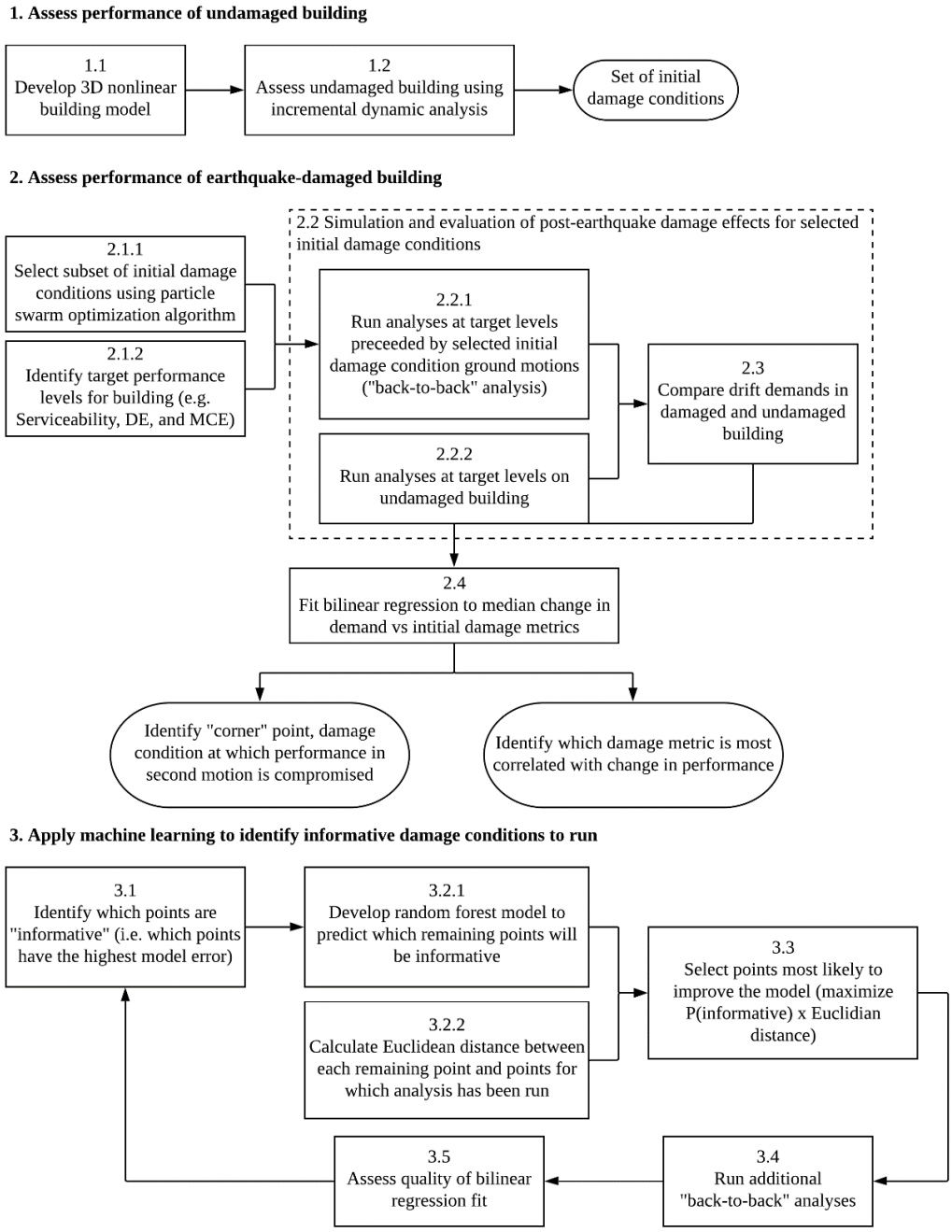

Fig. 1 – Overview of framework for assessment of the performance of an earthquake-damaged building in a subsequent event, using optimization and machine learning.

A three-dimensional nonlinear model of the building was developed in *OpenSees* [21]. This model employs lumped plasticity for beam and column elements. This approach is chosen for computational efficiency and for its advantages in capturing softening behavior with an appropriate hinge model [22]. At each beam-column interface, the panel zone was modeled with nearly rigid, elastic elements that represent joint size. These joint elements were connected to the elastic frame elements by zero-length hinges modeled using the Ibarra Medina Krawinkler (IMK) peak-oriented hysteretic model [23,24] to represent beam and column hinging behavior. The model considers cracked stiffness properties for beams and columns. A backbone curve for one of the columns (shown in Fig. 2b); backbone/cyclic deterioration parameters were determined using the calibration framework described by Haselton et al. [22]. These components are highly ductile.

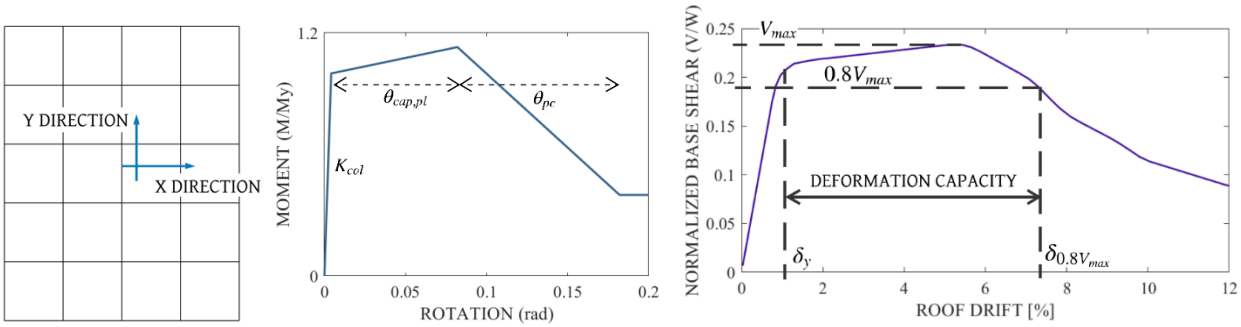

Fig. 2 – a) Plan view of building. b) Backbone curve of typical column in example building model. c) Static pushover of example building in weaker (x) direction in its undamaged state.

4. Assess performance of undamaged building

4.1 Initial damage conditions

In the first phase of the framework, the performance of the undamaged building is evaluated (Box 1.2). The goal of this assessment is to quantify the response of the structure under a variety of earthquake events. For each analysis (i.e., each ground motion and intensity measure), the response of the structure during dynamic analysis is quantified in terms of peak story and roof drifts, and residual drift.

In our example illustration, each dynamic analysis step consists of one of the pairs of FEMA P-695 far-field ground motions [19], scaled to increasing shaking intensities until a collapse threshold—10% story drift [5,25]—is reached. Shaking intensity is quantified in terms of geometric mean of spectral acceleration at the fundamental period of the building.

An example story drift time history is displayed in Fig. 3. During the analysis, peak story drift is measured as the maximum drift experienced in any story at any time during the ground motion. Peak roof drift is the highest overall building drift during the ground motion in both orthogonal directions. Residual drift is the highest drift in either direction that remains in a story at the end of the ground motion.

At the end of each ground motion, the period of the damaged building was calculated using eigenvalue analysis. The building was also subjected to a static pushover in the x direction following dynamic analysis. This pushover provided measures damaged building strength and deformation capacity of the building after each initial condition ground motion. Fig. 4 shows the pushover response of the damaged building after the same ground motion at different shaking intensities. The damaged building's strength is derived from the maximum base shear during the post-dynamic pushover divided by the building weight. The deformation capacity is the ratio of the displacement at 80% of the maximum base shear to the yield displacement.

Each IDC is based on one of these analyses. An IDC is defined by the ground motion and intensity at which it was applied, and has an associated suite of damage metrics including: peak story drift, peak roof drift, residual drift, change in strength (measured from pushover), change in stiffness (measured as the increase in fundamental period), and change in deformation capacity (also measured from pushover analysis). Fig. 5 provides an overview of the range of damage conditions of the example building under various ground motions.

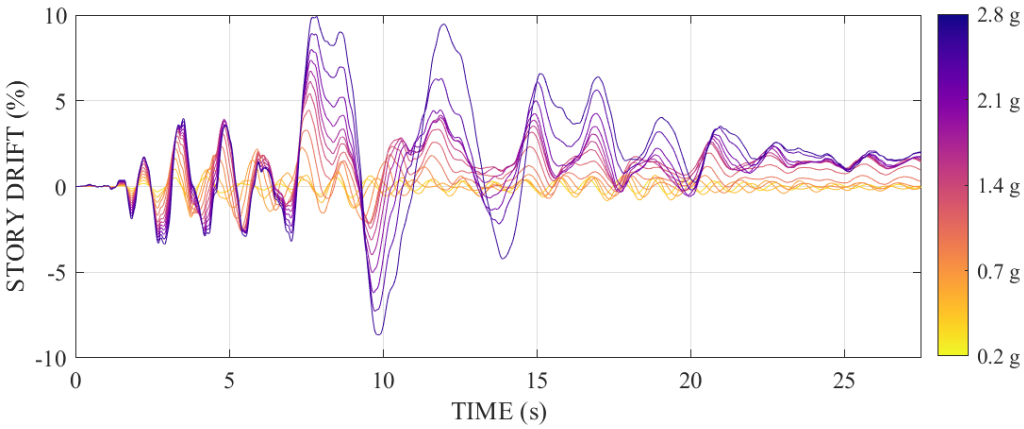

Fig. 3 – Story drift time history in the x-direction of the undamaged building at the second story simulated during ground motions of increasing shaking intensity for a ground motion recorded from 1971 San Fernando Earthquake at the Hollywood station.

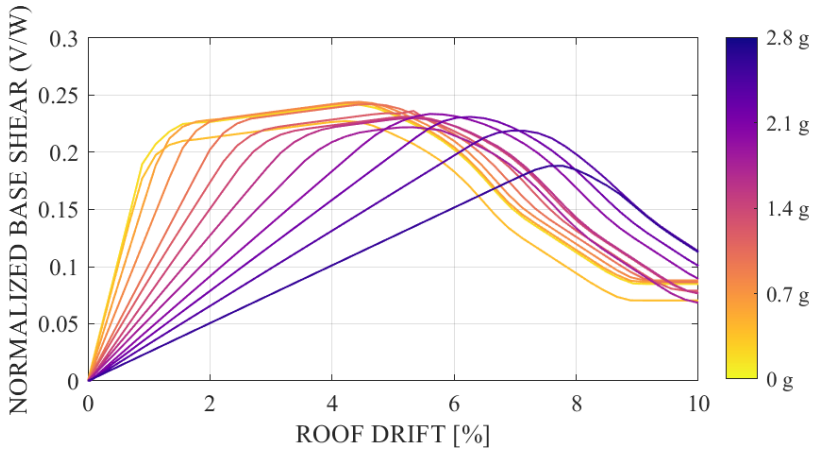

Fig. 4 – Static pushover response of the building in the x-direction, simulated after ground motions of increasing shaking intensity for a ground motion recorded from 1971 San Fernando Earthquake at the Hollywood station.

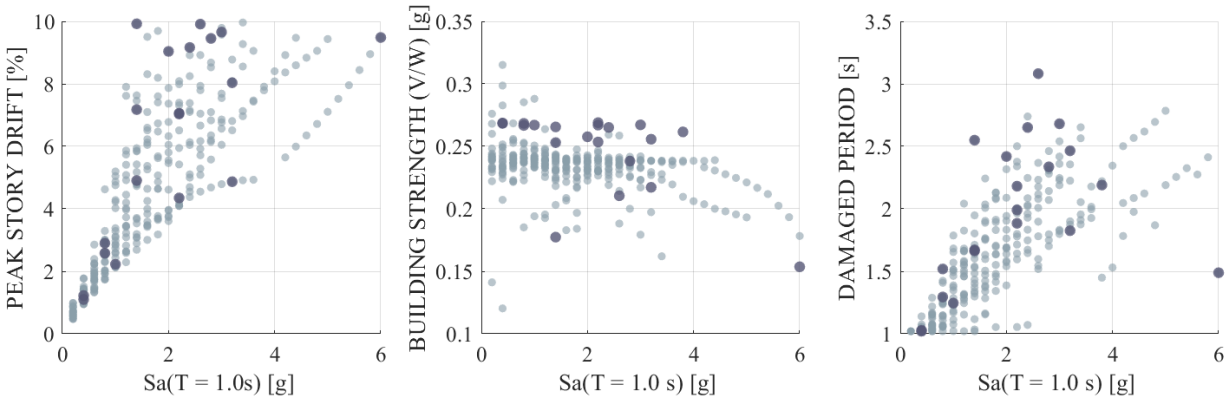

Fig. 5 – Summary of example undamaged building response in terms of a) peak story drift, b) post-earthquake strength and c) damaged building period at different shaking intensities. Each point represents an IDC; IDCs selected for subsequent analysis are darker circles. All responses are in x-direction.

5. Assess performance of earthquake-damaged building

5.1 Select subset of IDCs using particle swarm optimization algorithm

We first identified an initial set of 20 IDCs that is representative of all the IDCs using the Particle Swarm Optimization (PSO) algorithm [26]. This method employs an optimization algorithm that maximizes the distance between the points based on specified input parameters. In this case, the input parameters are damaged building strength, damaged building stiffness, residual drift after the first motion, and peak story drift in the initial damaging motion. These parameters are selected to ensure that the selected IDCs vary in terms of various damage metrics of interest; the selected IDCs are identified in Fig. 5.

5.2 Identify target performance levels for subsequent analyses

Of particular interest is the performance of the damaged buildings at target intensity levels: the Maximum Considered Earthquake (MCE), Design Earthquake (DE), and Serviceability. We used the USGS Unified Hazard Tool [27] to identify the target intensity levels appropriate for the selected building site. For this study, the MCE motion corresponds to a return period of 2,475 years, and the DE motion corresponds to a return period of 475 years.

The intensity of a ground motion for serviceability assessment is generally not well defined. Moehle et al. [28] suggest consideration of building occupant comfort. Dymiotis-Wellington and Vlachaki [29] consider the performance of structural and nonstructural building elements. Although not addressed explicitly or quantitatively in the American standards [30], these objectives are typically met by limiting story drifts. Dymiotis-Wellington and Vlachaki [29], for example, offers drift limits ranging from 0.5 – 1.0% depending on the nature of the building. The serviceability of a structure can alternatively be defined based on the return period of an earthquake. For example Wen [31] and PEER [32] assess serviceability with an earthquake corresponding to a44 and 43-year return periods. Serviceability ground motion is associated with a 100-year return period in Eurocode 8 [33]. The return period adopted for serviceability in the example illustration is 150 years, which is at the upper bound of values used in the literature.

For the example building, these levels were identified for a site in California the target ground motion intensities were 0.20 g for serviceability, 0.39 g for DE, and 0.86 g for MCE. The ground motion selection algorithm developed by Baker and Lee [34,35] was employed to identify twelve motions that matched the conditional mean spectrum for the building site for each level based on the hazard deaaggregation from the USGS [27]. These motions were scaled to the target serviceability, DE, and MCE levels based on the spectral acceleration at the fundamental period.

5.3 Simulation and evaluation of post-earthquake damage for selected IDCs

Fig. 6 illustrates the roof displacement time history of the building during each of the twelve analyses for one of the IDCs for the DE level. In each analysis, the building is subjected to the initial damaging motion (recreating the damage state) and one of the scaled subsequent motions.

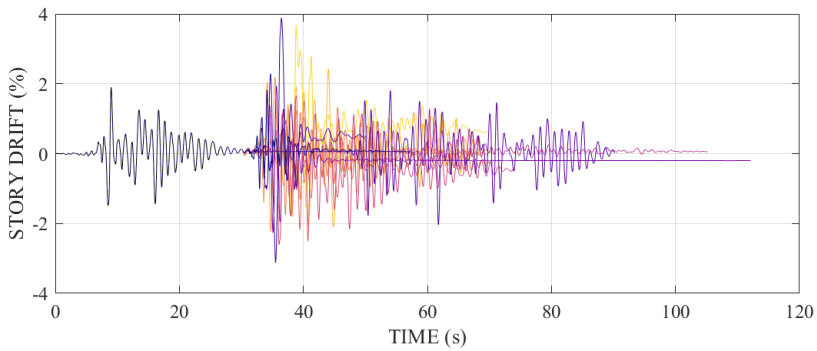

Fig. 6 – Story drift time histories in the x-direction of the example building subjected to one IDC and twelve subsequent motions scaled to the selected MCE level.

The response parameter of interest is the ratio in peak story drift demand during the motion in the damaged building as compared to the undamaged building in the same serviceability, DE, or MCE motion. The median ratio (over all the records) demands in the damaged to undamaged building quantifies the response for each IDC. We then plotted all of the IDCs with the peak story drift experienced in the initial motion on the x-axis and median change in drift demand on the y-axis and fit a bilinear regression to the data. This relationship is shown in Fig. 7 for the initially selected IDCs.

We fit a bilinear regression curve to the results obtained from analysis of the first 20 IDCs, as shown in Fig. 7. The choice of the bilinear fit was based on the observation that the demands on the building are generally unchanged for low levels of damage, but, past some point, increase steadily as the building experiences damage. The value identified as "corner" on these plots is the damage level at which the response starts to change. This regression was fit with the assumption that the value below the corner is 1 (i.e., the response of the damaged and undamaged building is the same). The figure shows that the bilinear regression is a good fit to the data; the R^2 values are reported in Fig. 8.

6. Apply machine learning to identify informative damage conditions to run

This framework employs a machine learning methodology developed by Bullock et al. [36] to improve computational efficiency. In this methodology, additional IDCs are selected for analysis based on the estimated probability that they will be informative. Informative IDCs are identified from analysis of the initial set as the IDCs that have a high influence on the bilinear regression parameters.

Determination of what IDCs were informative proceeds as follows. For each IDC in our bilinear regression, the model error was calculated as the observed ratio between median ratio of damaged to undamaged peak story drift from the simulation. minus the value predicted by the model. In this framework, points were identified as informative if the model error for a given point (i.e., IDC) was larger than the 75th percentile. This threshold ensures that the database is balanced (i.e., there are both informative and non-informative points) and a classifier can be fit to the data. The probability that a point from the remaining data (in this case, IDCs) will be informative is predicted by training a random forest [37] using the points classified as informative or not informative from the initial subset. The points identified as informative in the example are shown in Fig. 7.

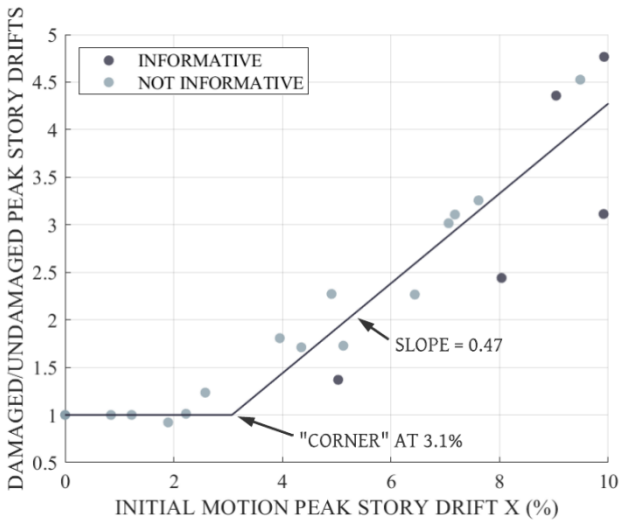

Fig. 7 – Median ratio of drift demand in damaged to undamaged building for each IDC for the DE level. These data are fit to a bilinear regression, and IDCs with the highest model error are noted as “informative”.

The regression model is improved by running additional IDCs. The additional points or IDCs are selected based on their likelihood of improving the model. This is based on the probability that point will be

informative, P(informative), multiplied by the minimum Euclidean distance between each potential point and the points from the initial subset in parameter space [36].

In all cases, the peak story drift experienced in an initial damaging ground motion was strongest predictor of performance in a subsequent motions. This observation is consistent with past research, where drift demand indicative of the remaining capacity of a structure in a subsequent event [8,11,17,38–40]. Fig. 8a reports the goodness of the bilinear regression model fit when different damage metrics are selected. In general, the drift measures were the strongest predictor of post-earthquake performance, with residual and roof drifts R^2 values exceeding 0.8.

We noted the quality of bilinear model fit as additional analyses were run; these values are displayed in Fig. 8b-c. IDCs were selected based on the likelihood that they would inform the model, and points were identified as informative if they had large error. Thus, it is logical that the model fit, quantified by the R^2 value, is largely unchanged as the number of analyses increases. The corner point (i.e., damage threshold) changes as additional analyses are included in the model, but the value tends to remain steady after approximately 30 analyses have been run. The slope trends similarly.

This method allows us to run fewer analyses than would be necessary using the "brute force" "back to back" method, where all IDCs are analyzed. The computational time to run 20 IDCs—6% of total ICDs—through one level of subsequent analysis requires approximately 24 hours of computational time. As is evident in Fig. 8b, the results remain largely unchanged as the number of analyses increases past 30 IDCs.

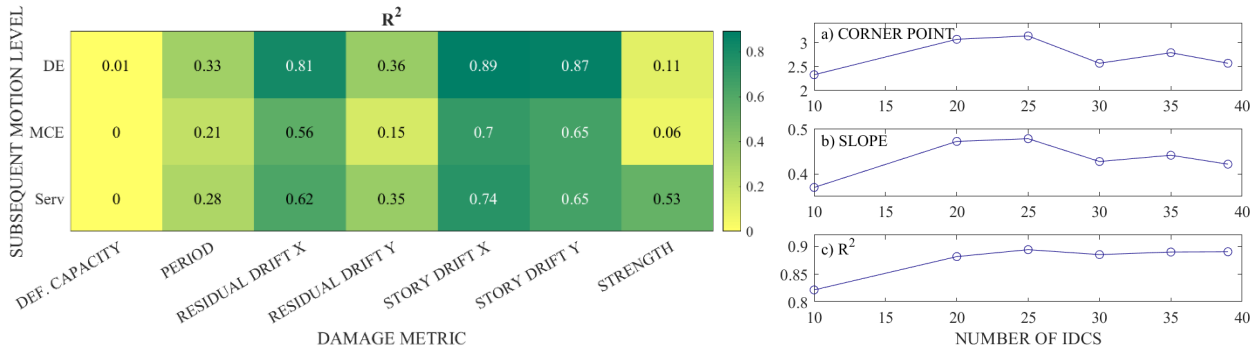

Fig. 8 – a) R^2 values for various damage metrics and target performance levels. b) Progression of bilinear model fit for DE level analyses showing regression parameters and goodness of fit as additional analyses are run. The corner and slope are defined on Fig. 7.

7. Results

In total, 50 IDCs were assessed for the example building's performance at serviceability level (Sa(T=1.0s) = 0.2 g) demands. The median drift in the undamaged building case at this scale is 0.5% drift. As Fig. 9 shows, the damaged building response is roughly equivalent to the undamaged building response below approximately 2.5% initial motion peak story drift. In this case, the building did not sustain damage significant enough during the initial motion to affect the response.

A similar trend emerged for DE level shaking, for which 39 IDCs were analyzed. In this case, the change in drift demand for a damaged building occurs around 3% initial motion peak story drift. The response below this threshold was virtually the same in the damaged building as in the undamaged one. In MCE level shaking, the effect of damage is not pronounced until the initial damage level reaches 5% drift. The ratio increases more sharply in serviceability cases than in DC and MCE cases.

These results taken together, this building is not very sensitive to damage for serviceability, DE, or MCE response until significant drift demands have been reached. This building is a ductile and strong system with a deformation capacity of column hinges close to 10% story drift (Fig. 2b). When damage is small (drifts on the order of 2-3%), there is substantial remaining energy dissipation capacity in the building/components and

the demands are unchanged in the second motion. This occurs even though the building period has elongated, increasing displacement demands, but reducing spectral energy input. The MCE level shaking performance is least sensitive to damage because its performance depends mostly on energy dissipation. In other words, response at serviceability levels tends to be dictated by stiffness, whereas the change in response at MCE and collapse levels is affected by cyclic deterioration. These trends are consistent with research by past research on the response of ductile buildings in multiple earthquake events [5,9,17]. We anticipate further investigation of the influence of subsequent motion intensity on damage threshold through application of this framework to additional buildings.

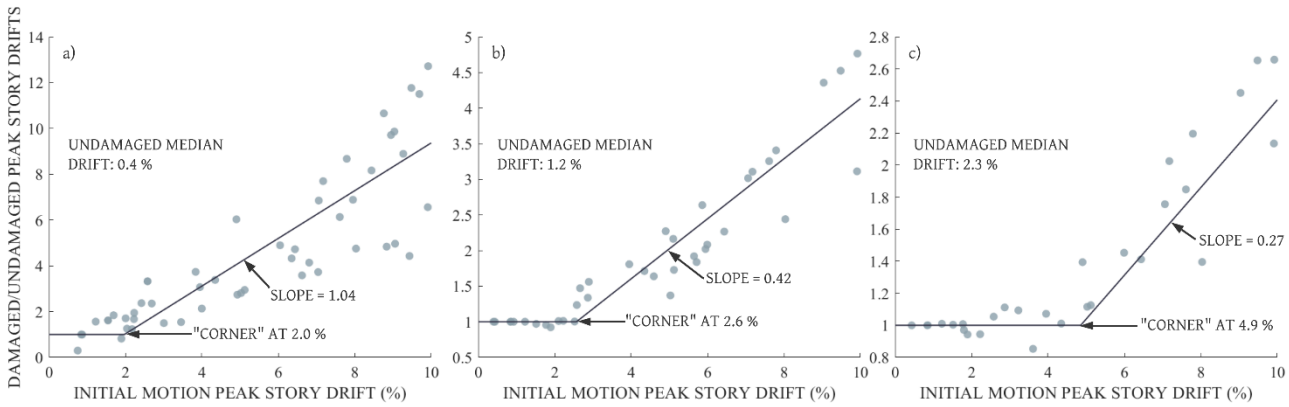

Fig. 9 – Median ratio drift demand in damaged to undamaged building for each IDC at a) serviceability, b) DE, and c) MCE level motions versus the peak story drift experienced during the initial damaging motion.

8. Conclusions

This framework was developed to identify which measures of damage best predict future earthquake performance of a ductile RC frame building, and to assess when damage is substantive enough to meaningfully affect future performance. The framework is illustrated through application to a modern, ductile, RC frame building. Physically, the results show that a "corner" damage condition threshold can be identified after which damage has an important influence on earthquake performance. The corner drift levels for this building are about 2%, 3% and 5% drift for serviceability, DE and MCE. These are roughly 20, 30 and 50% of the building deformation capacity. This example run also identified peak story drift as a strong indicator of future building performance. Methodologically, the framework was able to identify distinct changes in performance that are tied to reparability without undue computational burden. The machine learning based point selection algorithm selected points to efficiently improve the analysis set. The total analysis time is less than one week, whereas a similar level of detail using a brute force method would require several months of computational time on the same computer.

Further work will include the assessment of structures with structural irregularities, nonductile frames, and older structures. This expanded work will allow researchers to identify not only damage metrics that predict future performance, but also which building characteristics most affect performance and the limiting damage values.

9. Acknowledgments

The work forming the basis for this publication was conducted pursuant to a contract with the Federal Emergency Management Agency (FEMA) on the ATC 145 project. We gratefully acknowledge the input of others on the Project Technical Committee. The substance of such work is dedicated to the public. The author(s) are solely responsible for the accuracy of statements or interpretations contained in this publication. No warranty is offered with regard to the results, findings and recommendations contained herein, either by the FEMA, or the Applied Technology Council, its directors, members or employees. These organizations

and individuals do not assume any legal liability or responsibility for the accuracy, completeness, or usefulness of any of the information, product or processes included in this publication.

10. References

[1] Marquis, F., Kim, J. J., Elwood, K. J., & Chang, S. E. (2017). Understanding post-earthquake decisions on multi-storey concrete buildings in Christchurch, *New Zealand. Bulletin of Earthquake Engineering, 15*(2), 731-758.

[2] Marder, K., Elwood, K. J., Motter, C. J., & Clifton, G. C. (2019). Post-Earthquake Assessment of Moderately-Damaged Reinforced Concrete Plastic Hinges. *Earthquake Spectra*.

[3] Kam, W. Y., Pampanin, S., & Elwood, K. (2011). Seismic performance of reinforced concrete buildings in the 22 February Christchurch (Lyttelton) earthquake. *Bulletin of the New Zealand Society for Earthquake Engineering, 44*(4), 239-278.

[4] Elwood, K., Marquis, F., & Kim, J. H. (2015). Post-Earthquake Assessment and Repairability of RC Buildings: Lessons from Canterbury and Emerging Challenges. In *10th Pacific Conference on Earthquake Engineering.* Australian Earthquake Engineering Society (AEES).

[5] Raghunandan, M., Liel, A. B., & Luco, N. (2015). Aftershock collapse vulnerability assessment of reinforced concrete frame structures. *Earthquake Engineering & Structural Dynamics, 44*(3), 419-439.

[6] Hosseinpour, F., & Abdelnaby, A. E. (2017). Fragility curves for RC frames under multiple earthquakes. *Soil Dynamics and Earthquake Engineering, 98*, 222-234.

[7] Zhang, Y., Burton, H. V., Sun, H., & Shokrabadi, M. (2018). A machine learning framework for assessing post-earthquake structural safety. *Structural safety*, *72*, 1-16.

[8] Jeon, J. S., DesRoches, R., Lowes, L. N., & Brilakis, I. (2015). Framework of aftershock fragility assessment–case studies: older California reinforced concrete building frames. *Earthquake Engineering & Structural Dynamics, 44*(15), 2617-2636.

[9] Ryu, H., Luco, N., Uma, S. R., & Liel, A. B. (2011). Developing fragilities for mainshock-damaged structures through incremental dynamic analysis. In *9th Pacific Conference on Earthquake Engineering, Auckland, New Zealand*.

[10] Ruiz-García, J., & Aguilar, J. D. (2015). Aftershock seismic assessment taking into account postmainshock residual drifts. *Earthquake Engineering & Structural Dynamics*, *44*(9), 1391-1407.

[11] Li, Y., Song, R., Van de Lindt, J., Nazari, N., & Luco, N. (2012). Assessment of wood and steel structures subjected to earthquake mainshock-aftershock. In *15th world conference on earthquake engineering, Lisbon, Portugal*.

[12] Fairhurst, M., Bebamzadeh, A., & Ventura, C. E. (2019). Effect of Ground Motion Duration on Reinforced Concrete Shear Wall Buildings. *Earthquake Spectra*, *35*(1), 311-331.

[13] Raghunandan, M., & Liel, A. B. (2013). Effect of ground motion duration on earthquake-induced structural collapse. *Structural Safety*, *41*, 119-133.

[14] Chandramohan, R., Baker, J. W., & Deierlein, G. G. (2016). Quantifying the influence of ground motion duration on structural collapse capacity using spectrally equivalent records. *Earthquake Spectra*, *32*(2), 927-950.

[15] Mahin, S. A. (1980). Effects of duration and aftershocks on inelastic design earthquakes. In *Proceedings of the 7th world conference on earthquake engineering* (Vol. 5, pp. 677-680).

[16] Uma, S. R., Ryu, H., Luco, N., Liel, A. B., & Raghunandan, M. (2011). Comparison of main-shock and aftershock fragility curves developed for New Zealand and US buildings. In *Proceedings of the ninth pacific conference on earthquake engineering structure building and Earthquake-Resilient Society, Auckland, New Zealand* (pp. 14-16).

[17] Amadio, C., Fragiacomo, M., & Rajgelj, S. (2003). The effects of repeated earthquake ground motions on the non-linear response of SDOF systems. *Earthquake engineering & structural dynamics*, *32*(2), 291-308.

[18] Ramirez, C. M., Liel, A. B., Mitrani-Reiser, J., Haselton, C. B., Spear, A. D., Steiner, J., Deierlein, G., & Miranda, E. (2012). Expected earthquake damage and repair costs in reinforced concrete frame buildings. *Earthquake Engineering & Structural Dynamics*, *41*(11), 1455-1475.

[19] FEMA (2009). FEMA P-695: Quantification of building seismic performance factors. prepared by Applied Technology Council for the Federal Emergency Management Agency, Washington, D.C.

[20] Haselton, C. B., Liel, A. B., Deierlein, G. G., Dean, B. S., & Chou, J. H. (2011). Seismic collapse safety of reinforced concrete buildings. I: Assessment of ductile moment frames. *Journal of Structural Engineering*, *137*(4), 481-491.

[21] McKenna, F., Scott, M. H., & Fenves, G. L. (2010). Nonlinear finite-element analysis software architecture using object composition. *Journal of Computing in Civil Engineering*, *24*(1), 95-107.

[22] Haselton, C. B., Liel, A. B., Taylor-Lange, S. C., & Deierlein, G. G. (2016). Calibration of Model to Simulate Response of Reinforced Concrete Beam-Columns to Collapse. *ACI Structural Journal*, *113*(6).

[23] Ibarra, L. F., & Krawinkler, H. (2005). *Global collapse of frame structures under seismic excitations* (pp. 29-51). Berkeley, CA: Pacific Earthquake Engineering Research (PEER) Center.

[24] Ibarra, L. F., Medina, R. A., & Krawinkler, H. (2005). Hysteretic models that incorporate strength and stiffness deterioration. *Earthquake engineering & structural dynamics*, *34*(12), 1489-1511.

[25] Burton, H. V., Sreekumar, S., Sharma, M., & Sun, H. (2017). Estimating aftershock collapse vulnerability using mainshock intensity, structural response and physical damage indicators. *Structural safety*, *68*, 85-96.

[26] Kennedy, J., & Eberhart, R. (1995). Particle swarm optimization. In *Proceedings of ICNN'95-International Conference on Neural Networks* (Vol. 4, pp. 1942-1948). IEEE.

[27] United States Geological Society (USGS). "Unified Hazard Tool.". earthquake.usgs.gov/hazards/interactive/.

[28] Moehle, J., Bozorgnia, Y., & Yang, T. Y. (2007). The tall buildings initiative. In *Proceedings of SEAOC Convention, Squaw Creek, CA, USA* (pp. 315-324).

[29] Dymiotis-Wellington, C., & Vlachaki, C. (2004). Serviceability limit state criteria for the seismic assessment of RC buildings. In *Proceedings of the 13th World Conference on Earthquake Engineering. Vancouver, BC* (pp. 1-10).

[30] Uang, C. M., & Bertero, V. V. (1991). UBC seismic serviceability regulations: Critical review. *Journal of Structural Engineering*, *117*(7), 2055-2068.

[31] Wen, Y. K. (2001). Reliability and performance-based design. *Structural safety*, *23*(4), 407-428.

[32] Pacific Earthquake Engineering Research (PEER) Center. (2010). *Guidelines for performance-based seismic design of tall buildings*. PEER Center, College of Engineering, University of California.

[33] European Committee for Standardization. (2005). Eurocode 8: Design of structures for earthquake resistance.

[34] Baker, J. W., & Lee, C. (2018). An improved algorithm for selecting ground motions to match a conditional spectrum. *Journal of Earthquake Engineering*, *22*(4), 708-723.

[35] Baker, J. W. (2011). Conditional mean spectrum: Tool for ground-motion selection. *Journal of Structural Engineering*, *137*(3), 322-331.

[36] Bullock Z, Dashti S, Liel, A. B., & Porter K. (2019). A Framework for Machine Learning-Assisted Design and Execution of Numerical Parametric Studies in Evaluating the Seismic Response of Soil-Structure Systems. In *Proceedings of the 12th Canadian Conference on Earthquake Engineering, Quebec City, QC.*

[37] Liaw, A., & Wiener, M. (2002). Classification and regression by randomForest. *R news*, *2*(3), 18-22.

[38] Goda, K., & Salami, M. R. (2014). Inelastic seismic demand estimation of wood-frame houses subjected to mainshock-aftershock sequences. *Bulletin of Earthquake Engineering*, *12*(2), 855-874.

[39] Aoki, Y., Ohashi, Y., Fujitani, H., Saito, T., Kanda, J., Emoto, T., & Kohno, M. (2000). Target seismic performance levels in structural design for buildings. In *Proceedings of 12th World Conference of Earthquake Engineering, Ed. CD-ROM, Nueva Zelanda*.

[40] Hosseinpour, F., & Abdelnaby, A. E. (2017). Effect of different aspects of multiple earthquakes on the nonlinear behavior of RC structures. *Soil Dynamics and Earthquake Engineering*, *92*, 706-725.